

A Method to Calculate Homoclinic Points of a Two-Dimensional Noninvertible Map

Tetsuya YOSHINAGA[†], Hiroyuki KITAJIMA[†], Hiroshi KAWAKAMI[†], *Members,*
and Christian MIRA^{††}, *Nonmember*

SUMMARY A numerical method is presented for calculating transverse and non-transverse (or tangent) types of homoclinic points of a two-dimensional noninvertible map having an invariant set that reduces to a one-dimensional noninvertible map. To illustrate bifurcation diagrams of homoclinic points and transitions of chaotic states near the bifurcation parameter values, three systems including coupled chaotic maps are studied.

key words: noninvertible map, homoclinic point, bifurcation, coupled map, nonlinear problem

1. Introduction

Recently there are many investigations on coupled discrete maps [1]–[3], which are considered as models of coupled oscillators derived from physical systems. Several phenomena observed in coupled chaotic oscillators can be reproduced by a coupling of one-dimensional noninvertible maps. Using a model described by discrete dynamical system, we may clarify mechanisms of generation of chaos, transition or bifurcation of chaos, chaotic synchronization and so on.

The appearance of homoclinic structure in dynamical systems is a global phenomenon and important on the occurrence of chaotic behavior. There is, however, no direct method to obtain homoclinic solutions for a general noninvertible map. On the other hand, it is possible to calculate homoclinic solutions and their bifurcation set for forced differential equations as well as invertible maps [6], [7]. In this paper, we propose a computational method to calculate homoclinic solutions of a noninvertible map for a special case.

We consider a discrete map as a function of a real parameter vector λ , defined by

$$T_\lambda : R^2 \rightarrow R^2; (x, y) \mapsto (x', y') \quad (1)$$

where the system has an invariant set such that the restriction to the line $px + qy = r$ ($p^2 + q^2 \neq 0$) reduces to a one-dimensional noninvertible map. We also suppose that Eq. (1) has a saddle type of fixed or periodic point, say D_0 , on the line $px + qy = r$, and a homoclinic point Q_0 exists as an intersection of α - and ω -branches (or

unstable and stable sets, respectively) of the point D_0 . Moreover we treat a special case where the ω -branch is restricted to the invariant set $px + qy = r$, so the point Q_0 is located on the line, although the ω -branch itself may be folded. Indeed, this situation is typically observed in, e.g., a coupling of identical chaotic maps as shown in Sect. 4 and this phenomenon is related to a transition of chaos with a symmetric property. From the above assumption, we can obtain the point Q_0 using a similar computational method for invertible maps, because it is not necessary to calculate the ω -branch of the noninvertible map.

2. Method

In this section, we show methods for calculating transverse and non-transverse (or tangent) types of homoclinic solutions. The two situations are sketched in Fig. 1. Note that a periodic point with period k can be studied by replacing T_λ with T_λ^k , k -th iterates of T_λ , in Eq. (1). Therefore in the following we consider only homoclinic point of the fixed point of T_λ . Similar argument can be applied to the periodic point of T_λ .

2.1 Transverse Type of Homoclinic Point

We first consider a method for obtaining a transverse type of homoclinic point Q_0 using a local representation of α -branch. Let the point D_0 be a saddle type of

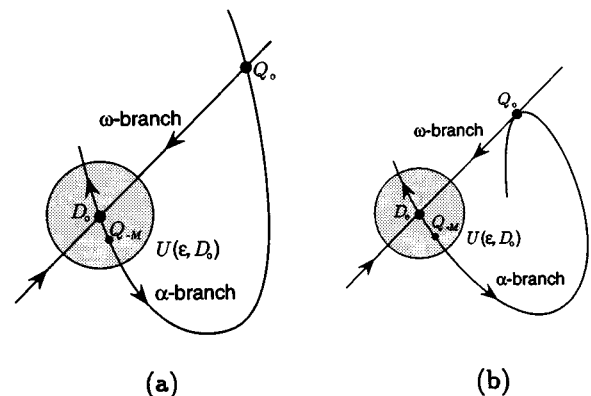


Fig. 1 Schematic diagrams for (a) transverse and (b) non-transverse (or tangent) types of homoclinic points.

Manuscript received January 31, 1997.

[†]The authors are with the Faculty of Engineering, Tokushima University, Tokushima-shi, 770 Japan.

^{††}The author is with Institut National des Sciences Appliquées de Toulouse, Avenue de Rangueil, 31077 Toulouse Cedex, France.

fixed point:

$$T_\lambda(D_0) - D_0 = 0 \tag{2}$$

We take an ε -neighborhood $U(\varepsilon, D_0)$ as shown in Fig. 1 (a), then there exists a positive integer M such that

$$T_\lambda^M(Q_{-M}) = Q_0, \quad Q_{-M} \in U(\varepsilon, D_0) \tag{3}$$

Because Q_0 is on the line $px + qy = r$, the point Q_{-M} satisfies

$$(p \ q) T_\lambda^M(Q_{-M}) - r = 0 \tag{4}$$

Hence the problem for obtaining the point Q_0 reduces to a problem to find the point Q_{-M} ($\in \alpha$ -branch) that satisfies Eq. (4) and is included in the region $U(\varepsilon, D_0)$.

Now, we use the first order approximation or eigen-vector as the local representation of α -branch in the ε -neighborhood. The condition such that the point Q_{-M} is included in the α -branch is written as

$$W_\alpha^*(Q_{-M} - D_0) = 0 \tag{5}$$

where the row vector W_α^* is

$$W_\alpha^* = \begin{pmatrix} 1 & 0 \\ 0 & 1 \end{pmatrix} (\mu_\alpha I - DT_\lambda), \text{ or} \tag{6}$$

In the equation, DT_λ indicates the derivative of T_λ with respect to the fixed point D_0 , and $|\mu_\alpha| > 1$ denotes the characteristic multiplier.

If the α -branch intersects the ω -branch or the line $px + qy = r$ at the point Q_0 , then Eq. (5) is independent of Eq. (4). Therefore we can determine variables $Q_{-M} \in R^2$ for the set of Eqs. (4) and (5), using, e.g., Newton's method.

2.2 Non-Transverse or Tangent Type of Homoclinic Point

Then we consider a homoclinic point such that the α -branch is tangent to the ω -branch (or the line $px + qy = r$) at the point Q_0 . This is a problem for obtaining a bifurcation of homoclinic motion.

The calculation is done by solving homoclinic point and an element of the parameter vector λ , say λ_1 , simultaneously, for equations of 2nd order tangent homoclinicity. Figure 1 (b) shows a schematic diagram for the situation. Let

$$\phi : R \rightarrow R^2; \quad s \mapsto \phi(s) \tag{7}$$

be a representation of the α -branch in $U(\varepsilon, D_0)$, where $\phi(0) = D_0$ and $\phi(s_\alpha) = Q_{-M}$.

We now consider the derivative of ϕ with respect to s , that is,

$$\frac{d\phi}{ds}(s) = W(\phi(s)) \tag{8}$$

then we have a tangent vector of the α -branch at the point Q_0

$$\left. \frac{d(T_\lambda^M \circ \phi)}{ds} \right|_{s=s_\alpha} = DT_\lambda^M(\phi(s_\alpha)) \frac{d\phi}{ds}(s_\alpha) = DT_\lambda^M(Q_{-M})W_\alpha \tag{9}$$

where $W(\phi(s_\alpha)) = W_\alpha$, for simplicity. Hence we have a condition for coincidence of the directions W_α and the line $px + qy = r$:

$$\det \left(DT_\lambda^M(Q_{-M})W_\alpha : \begin{pmatrix} -q \\ p \end{pmatrix} \right) = 0 \tag{10}$$

where W_α is a vector transposed to W_α^* , that is,

$$W_\alpha^T = W_\alpha^* \begin{pmatrix} 0 & 1 \\ -1 & 0 \end{pmatrix} \tag{11}$$

where T indicates the transpose. Hence the problem is reduced to determine variables $(D_0, Q_{-M}, \lambda_1) \in R^5$ for the set of Eqs. (2), (4), (5) and (10).

2.3 Algorithm for Obtaining Homoclinic Tangency

To obtain bifurcation diagram for homoclinic tangency, we can achieve the following algorithm:

- Step 1: Set appropriate first guess for a homoclinic point.
- Step 2: Solve transverse type of homoclinic point using the method stated in Sect. 2.1 and trace it by varying a system parameter while checking the tangent vector of α -branch at the homoclinic point. If the program stops or the left hand side of Eq. (10) approaches to zero, the values of the set (D_0, Q_{-M}, λ) should be used for initial values of the next step.
- Step 3: Solve variables (D_0, Q_{-M}, λ_1) for the non-transverse type of homoclinic point using the method stated in Sect. 2.2.
- Step 4: Change the value of another parameter $\lambda_2 \in \lambda$ by $\lambda_2 + \Delta$, where Δ is an appropriate small value, and return to Step 3.

In the case where it is necessary to obtain the first homoclinic tangency[†], Step 4 should be replaced by

- Step 4': If there is another transverse of α -branch to the line $px + qy = r$, then return to Step 2 for the transverse type of homoclinic point.

[†]The term 'first' means that there is no other homoclinic point except the unique tangency.

3. Definition and Notations of Bifurcations

Before showing numerical results concerning with homoclinic structure, we should summarize some definitions of local bifurcations of fixed and periodic points of general discrete map, and notations for bifurcation sets appeared in bifurcation diagrams.

The symbol ${}_kD^m$ (resp. ${}_kI^m$) denotes a hyperbolic periodic point such that D (resp. I) indicates a type with even (resp. odd) number of characteristic multipliers on the real axis $(-\infty, -1)$, k indicates the number of characteristic multiplier outside the unit circle in the complex plane, m indicates m -periodic point.

A local bifurcation occurs when the topological type of a periodic point is changed by the variation of system parameter λ [9], [10]. In the proceeding section we will observe generic codimension-one bifurcations of tangent (or fold), period-doubling (or flip) and the Neimark-Sacker bifurcations, and D -type of branching as a degenerate case of the tangent bifurcation. These bifurcations are observed when the hyperbolicity is destroyed, which corresponds to the critical distribution of the characteristic multiplier μ such that $\mu = +1$ for tangent and D -type of branching, $\mu = -1$ for period-doubling bifurcation, and $\mu = e^{j\theta}$ for the Neimark-Sacker bifurcation, where $j = \sqrt{-1}$. To calculate local bifurcations, we use the method proposed in Ref. [11].

In bifurcation diagram, we use notations:

- H_l^m for homoclinic tangency of m -periodic point,
- G_l^m for tangent bifurcation of m -periodic point,
- D_l^m for D -type of branching of m -periodic point,
- I_l^m for period-doubling bifurcation of m -periodic point, and
- N_l^m for the Neimark-Sacker bifurcation of m -periodic point,

where l denotes the number to distinguish several same sets of $()^m$, if they exist. If $m = 1$, it will be omitted.

4. Examples

We illustrate some numerical results of calculating homoclinic bifurcations showing several interesting phenomena related to a transition of chaos.

4.1 A Coupled System of Chaotic Neurons

The system of our first example is a coupling of two identical chaotic neurons [3]–[5]:

$$T_\lambda \left\{ \begin{pmatrix} x' \\ y' \end{pmatrix} = \begin{pmatrix} 0.8x + a - h(x) + wh(y) \\ 0.8y + a - h(y) + wh(x) \end{pmatrix} \right. \quad (12)$$

where

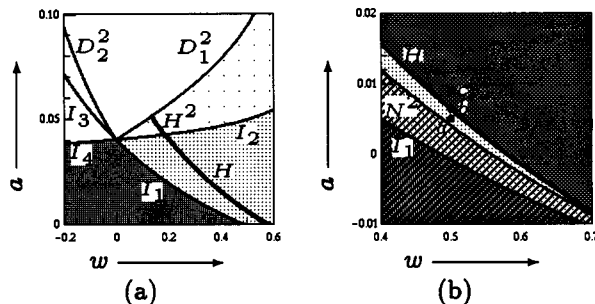



Fig. 2 Bifurcation diagrams for Eq. (12). Note that, in the figure (a), several bifurcation curves, e.g., the curve N^2 observed in the figure (b), are omitted for the simplicity.

$$h(u) = \frac{1}{1 + e^{-\frac{u}{0.03}}}$$

and $\lambda = (a, w)$. Note that the restriction to $x = y$ reduces to a one-dimensional system.

We obtain parameter sets of local and global bifurcations as shown in Fig. 2. In the region shaded by \blacksquare , there exists a stable fixed point satisfying $x \equiv y$. By passing through the curve I_1 from this region, we have ${}_1I$ -type of fixed point which exists in the region \square . When the system parameter varies from the region with shading \blacksquare through the curve I_2 , the following bifurcation is observed: ${}_1I \rightarrow {}_2D + 2 {}_1D^2$. The region \square shows the parameter values at which the 2-periodic point ${}_1D^2$ exists. Moreover, due to the variation of the system parameters, the point ${}_1D^2$ meets a D -type of branching denoted by the curve D_1^2 and then its stability changes to ${}_2D$ -type. In the parameter plane, we observe the intersections of both two curves of period-doubling bifurcations, I_1 – I_3 and I_2 – I_4 , and D -type of branchings, D_1^2 and D_2^2 , at the point satisfying $w = 0$ or without coupling. This phenomenon is typically observed in a coupling of two identical dynamical systems each of which has a period-doubling bifurcation [12]. A schematic diagram of manifolds for the fixed and 2-periodic points is shown in Fig. 3.

Now, each of the points ${}_1I$ and ${}_1D^2$ has an ω -branch on the line $x = y$, and, if only the fixed or 2-periodic saddle exists, the α - and ω -branches intersect each other and form a transverse type of homoclinic structure at every parameter point in the region shown in Fig. 2. The curve H in Fig. 2 denotes the parameter set on which a non-transverse type of homoclinic point of the fixed point ${}_1I$ appears. The curve is also schematically illustrated in Fig. 3. Phase portraits of attractors and α -branches of the fixed point observed at the parameter points a – c in Fig. 2 (b) are shown in Fig. 4, where the coordinate system is transformed by $u = (x + y)/\sqrt{2}$ and $v = (x - y)/\sqrt{2}$ to see the detail near the line $x = y$ or $v = 0$. In each phase portrait, the α -branch is drawn up to a first transverse with the ω -branch, and another α -branch that is symmetric with respect to the line $v = 0$ is omitted.

We have an attractive invariant closed curve of the iterations of Eq. (12) with parameter values indicated by the point *a*, see Fig. 4 (a). This invariant closed curve is generated by the Neimark-Sacker bifurcation, denoted by the curve *N*² in Fig. 2 (b), of a stable 2-periodic point with property *T*_λ(*x*, *y*) = (*y*, *x*), which exists in the region with shading . By increasing the value of the parameter *a* for fixed *w* = 0.5, at the point *b* or on the

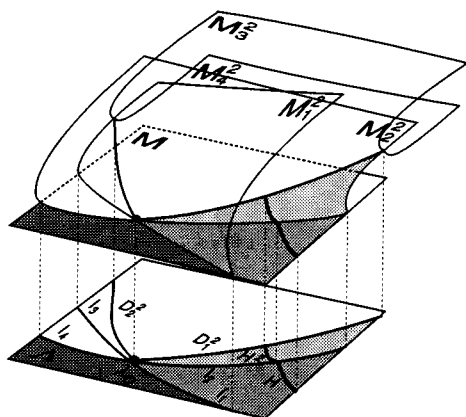


Fig. 3 Schematic diagram of fixed point manifold *M* and 2-periodic point manifolds *M*² for the intersection of two period-doubling bifurcation sets. The projection of the bifurcation conditions on the manifolds to the parameter plane Λ gives the bifurcation diagram.

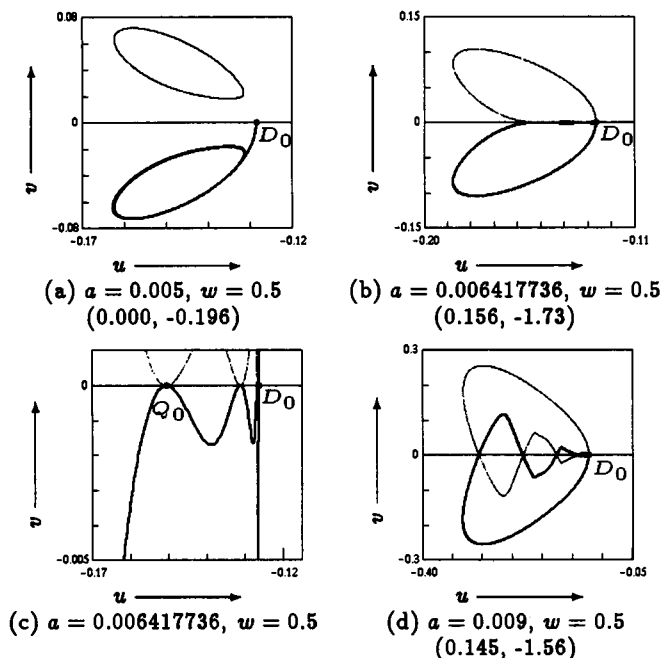
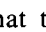


Fig. 4 Phase portraits for Eq. (12) in the transformed coordinate system. The point with symbol *D*₀ and the curve denote the fixed point and its α -branch, respectively. The points indicate an attractor without initial transition. Parameter values are denoted by the points (a) *a*, (b) *b*, and (d) *c* in Fig. 2 (b). The figure (c) is for an enlargement of (b). The values of the Lyapunov exponents appear in parentheses.


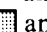
curve *H* in Fig. 2 (b), we observe a non-transverse type of homoclinic point as shown in Fig. 4 (b). The homoclinic point is indicated by the point *Q*₀ in Fig. 4 (c) showing an enlargement of Fig. 4 (b). When the homoclinic point becomes a transverse type, due to more increase of the parameter *a*, we see that the invariant closed curve changes to a chaotic attractor near the α -branch which forms the transverse homoclinic structure as shown in Fig. 4 (d), occurring at the point *c* in Fig. 2 (b). Therefore the curve *H* shows a bifurcation set for the transition between the invariant closed curve and the chaotic attractor. The parameter region in which the chaotic attractor exists is indicated by the shading  in Fig. 2 (b). Note that the attractor shown in Fig. 4 (d) is a characteristic chaos observed in the neuron model [3]. It is an advantage of our method to be able to obtain bifurcation parameters at which the chaos generates.

4.2 A Coupled Quadratic Map

As the second example, we see the first homoclinic tangency which is observed in the system composed by two identical quadratic maps [12]:

$$T_\lambda \left\{ \begin{pmatrix} x' \\ y' \end{pmatrix} = \begin{pmatrix} x^2 - \alpha - \delta(y - x) \\ y^2 - \alpha - \delta(x - y) \end{pmatrix} \right. \quad (13)$$

where $\lambda = (\alpha, \delta)$. The system of Eq. (13) is reduced to one-dimensional map when the condition *x* = *y* satisfies.

Figure 5 shows a bifurcation diagram for local and global bifurcations. In the figure, the line *I*² ($\alpha = 1.25$) shows a period-doubling bifurcation of 2-periodic point with property *x* \equiv *y*. By increasing the value of α through 1.25, the following bifurcation occurs: ${}_1I^2 \rightarrow {}_2D^2 + 2 {}_1D^4$. The bifurcated 4-periodic point ${}_1D^4$ also satisfies *x* \equiv *y*, which exists in the regions  and . Moreover its ω -branch is on the line *x* = *y*, and the eigenvector of the unstable characteristic multiplier is (1, -1). On the curve *H*⁴, we have a first homoclinic tangency of the α - and ω -branches

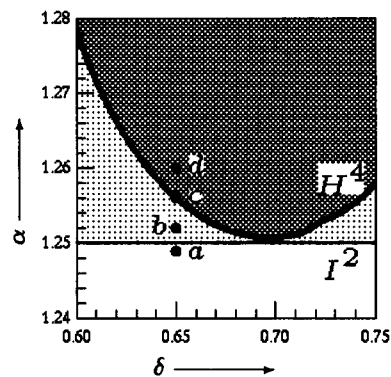


Fig. 5 Bifurcation diagram for Eq. (13).

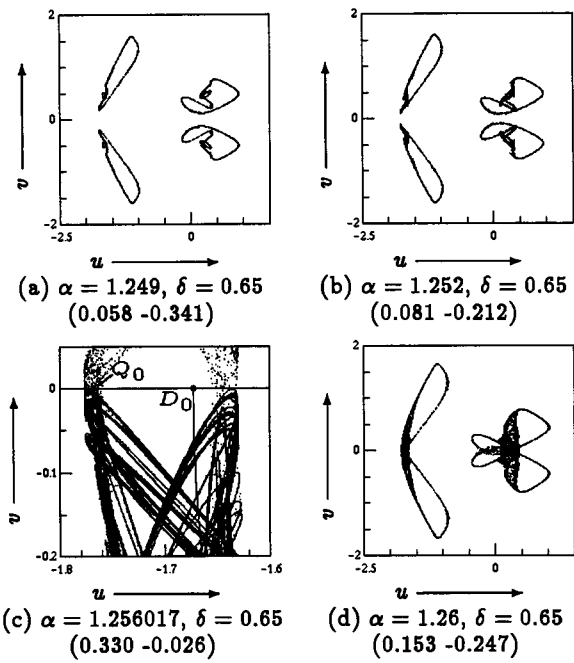


Fig. 6 Phase portraits for Eq. (13) in the transformed coordinate system. Parameter values are denoted by the points (a) *a*, (b) *b*, (c) *c*, and (d) *d*. The points indicate an attractor without initial transition. The values of the Lyapunov exponents appear in parentheses. In the figure (c), the point with symbol *D*₀ and the curve denote one of the periodic points and its α -branch, respectively, and note that another α -branch that is symmetric with respect to the line $v = 0$ is omitted. The point with symbol *Q*₀ indicates the first homoclinic point.

of the periodic point ${}_1D^4$. We have transverse type of homoclinic points of the periodic point ${}_1D^4$ only in the region shaded by ████.

Figures 6(a)–(d) show phase portraits in the transformed coordinate system (u, v) where $u = (x + y)/\sqrt{2}$ and $v = (x - y)/\sqrt{2}$. By continuous variation of the parameter α from the point *a* to the point *d* in Fig. 5, we have a transition between disconnected (Fig. 6(a) or (b)) and connected (Fig. 6(d)) chaotic attractors with respect to the line $v = 0$. The curve H^4 for first homoclinic tangencies separates the transition of two types of chaotic attractors. An example of phase portrait for the first homoclinic tangency is illustrated in Fig. 6(c) with chaotic attractor observed at the point *c* in Fig. 5. In the figure, the point *Q*₀ indicates the first homoclinic point of the periodic point *D*₀ after and before many self intersections of the α -branch.

4.3 A Two-Dimensional Version of Myrberg's Map

As the third example, we treat the system taken from Ref. [13]:

$$T_\lambda \left\{ \begin{pmatrix} x' \\ y' \end{pmatrix} = \begin{pmatrix} x^2 - y^2 - \alpha + \epsilon x \\ 2xy - 2.5\epsilon y \end{pmatrix} \right. \quad (14)$$

where $\lambda = (\alpha, \epsilon)$. This system is not invariant with re-

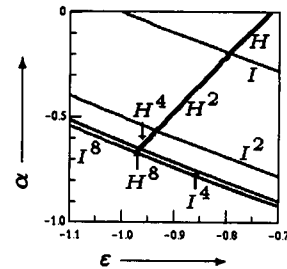


Fig. 7 Bifurcation diagram for Eq. (14).

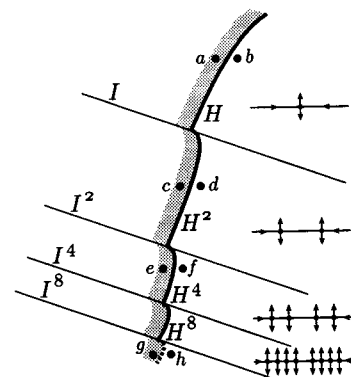


Fig. 8 Schematic diagram for Fig. 7. Bifurcation diagram in parameter plane $\lambda = (\epsilon, \alpha)$ and locations of periodic points on the line $y = 0$ are schematically shown.

spect to the replacement of state variables x and y , in comparison with the preceding two examples, and the restriction to $y = 0$ reduces to the Myrberg map.

Figure 7 is for showing bifurcations of first homoclinic tangencies, denoted by the thick curves with symbols H and H^m , of fixed and m -periodic points, where $m = 2, 4, 8$. The fixed and periodic points are observed on the line $y = 0$ and there is a doubling process of their period-doubling bifurcations indicated by the thin curves I and I^m , $m = 2, 4, 8$. We see that there exist successive occurrences of the homoclinic bifurcations together with the period-doubling bifurcations. The occurrence of the infinite doubling processes is conjectured. We shall show a schematic diagram for the doubling process of the homoclinic and period-doubling bifurcations, see Fig. 8. The points labeled by *a*–*h* are for indicating parameters at which chaotic attractors shown in Fig. 9 are observed. The periodic points on the line $y = 0$, which exist in regions separated by the period-doubling bifurcations are also schematically illustrated in the diagram. At the points *g* and *h*, we have chaotic states restricted to the set $y = 0$. In Fig. 9, phase portraits of attractors with and without homoclinic structures, which can be called as connected and disconnected chaotic attractors, respectively, are shown. The transition between the two types of chaotic attractors occurs on the curves of the first homoclinic tangencies.

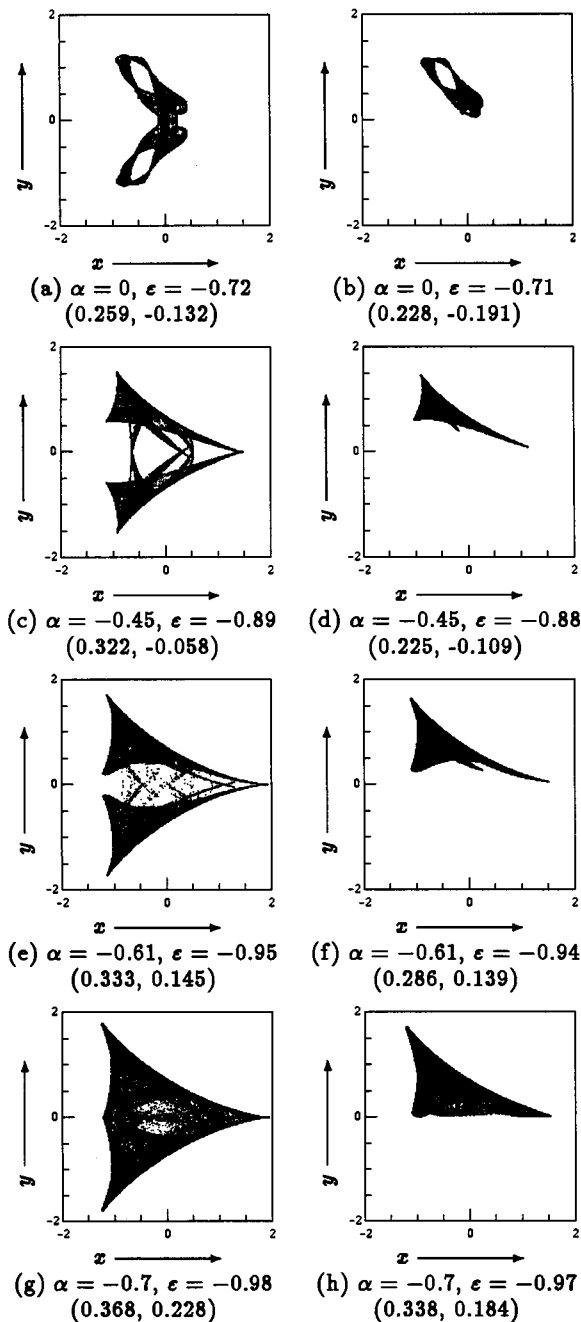


Fig. 9 Phase portraits for attractors observed in Eq. (14). Each attractor is observed at the parameter point with the same symbol in Fig. 8 as the figure label. Attractors with and without homoclinic structures are shown on the left ((a), (c), (e) and (g)) and right ((b), (d), (f) and (h)), respectively. Note that, for each figure on the right ((b), (d), (f) and (h)), another attractor that is symmetric with respect to the line $y = 0$ is omitted. The values of the Lyapunov exponents appear in parentheses.

5. Conclusion

Using the proposed method for obtaining homoclinic tangencies, the following results were obtained:

1. We obtained bifurcation parameter set that causes

the generation of a chaotic attractor, which is a characteristic chaos observed in a coupling of two identical chaotic neurons.

2. A mechanism of the transition between disconnected and connected chaotic attractors observed in a coupled quadratic map was clarified.
3. A doubling process of homoclinic structures together with period-doubling bifurcations was found in a two-dimensional version of Myrberg's map.

For the third example or the system of Eq. (14), a method for detecting the transition between disconnected and connected chaotic attractors was investigated [14] using the critical curve [15], [16], which is a method to analyze a chaotic behavior in the phase plane. The relation between critical curves and the first homoclinic tangency is a future interesting problem to be considered.

Finally we should note that although we only consider, in this paper, the case where the restriction to ω -branch is the line $px + qy = r$, it is possible to apply to more general case such as $h(x, y) = 0$, where h is a known C^∞ function.

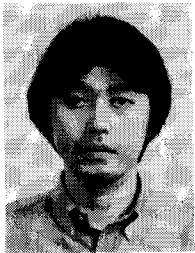
References

- [1] K. Kaneko, "Collapse of Tori and Genesis of Chaos in Dissipative Systems," World Scientific, 1986.
- [2] L. Gardini, R. Abraham, R. Record, and D. Fournier, "A double logistic map," *Int. J. Bifurcation and Chaos*, vol.4, no.1, pp.145-176, 1994.
- [3] K. Aihara, "Chaotic neural networks," in *Bifurcation Phenomena in Nonlinear Systems and Theory of Dynamical Systems*, ed. H. Kawakami, World Scientific, pp.143-161, 1989.
- [4] K. Judo, A.I. Mess, K. Aihara, and M. Toyoda, "Grid imaging for a two-dimensional map," *Int. J. Bifurcation and Chaos*, vol.1, no.1, pp.197-210, 1991.
- [5] M. Toyoda, "Chaotic neural networks," Master thesis of Tokyo Denki University, 1990.
- [6] H. Kawakami, *C.R. Acad. Sc. Paris*, 293, Série I, pp.401-403, 1981.
- [7] H. Kawakami and J. Matsuo, "Bifurcation of Doubly Asymptotic Motions in Nonlinear Systems," *IECE Trans.*, vol.J65-A, no.7, pp.647-654, 1982.
- [8] Y. Zhiping, J.K. Eric, and A.Y. James, "Calculating stable and unstable manifolds," *Int. J. Bifurcation and Chaos*, vol.1, no.3, pp.605-623, 1991.
- [9] N. Levinson, "Transformation theory of nonlinear differential equations of the second order," *Ann. Math.*, vol.45, pp.732-737, 1944.
- [10] K. Shiraiwa, "A generalization of the Levinson-Massera's equalities," *Nagoya Math.*, vol.67, pp.121-138, 1977.
- [11] H. Kawakami, "Bifurcation of periodic responses in forced dynamic nonlinear circuits: Computation of bifurcation values of the system parameters," *IEEE Trans. Circuits & Syst.*, vol.CAS-31, pp.248-260, 1984.
- [12] T. Yoshinaga, H. Kitajima, and H. Kawakami, "Bifurcations in a coupled Rössler system," *IEICE Trans.*, vol.E78-A, no.10, pp.1276-1280, 1995.

- [13] C. Mira and T. Narayaninsamy, "On behaviors of two-dimensional endomorphism: Role of critical curves," *Int. J. Bifurcation and Chaos*, vol.3, no.1, pp.187-194, 1993.
- [14] D. Fournier-Prunaret, C. Mira, and L. Gardini, "Some contact bifurcations in two-dimensional examples," *European Conference on Iteration Theory*, Sept. 1994.
- [15] C. Mira, "Détermination pratique du domaine de stabilité d'un point d'équilibre d'une récurrence nonlinéaire du deuxième ordre à variables réelles," *C.R. Acad. Sci. Paris*, vol.261, pp.5314-5317, 1965.
- [16] I. Gumowski and C. Mira, "Dynamique Chaotique," Cepadues Editions, Toulouse, 1980.



Christian Mira was born in Meknes, Morocco, on March 6, 1934. He received the B.Eng. degree from Ecole Nationale Supérieure d'Electrotechnique et d'Hydraulique de Toulouse (ENSEHT), Toulouse, France, in 1957, and "Doctorat es-Sciences Physiques" from Toulouse University, in 1961. Presently, he is a Professor of Control Engineering, Institut National des Sciences Appliquées (INSA), Département de Genie Electrique et Informatique, Toulouse, France. His interest is the qualitative theory of dynamical systems, chaotic dynamics, and their applications to engineering problems.

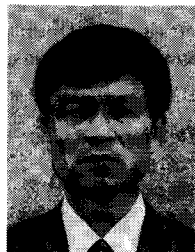


Tetsuya Yoshinaga was born in Tokushima, Japan, on April 23, 1961. He received the B.Eng. and M.Eng. degrees from Tokushima University, Tokushima, Japan, in 1984 and 1986, respectively, and the Dr.Eng. degree from Keio University, Yokohama, Japan, in 1992, all in electronic engineering. He was a Research Associate at School of Medical Sciences, Tokushima University and is an Associate Professor at Department of Electrical and

Electronic Engineering, Tokushima University, since 1996. Particularly, his current research interests are in bifurcation problems in nonlinear dynamical systems.



Hiroyuki Kitajima was born in Tokushima, Japan, on June 25, 1970. He received the B.Eng. and M.Eng. degrees in Electrical and Electronic Engineering from Tokushima University, in 1993 and 1995, respectively. He is presently working toward the Ph.D. degree at Tokushima University. His research interests include bifurcation problems. He is a JSPS Research Fellow.



Hiroshi Kawakami was born in Tokushima, Japan, on December 6, 1941. He received the B.Eng. degree from Tokushima University, Tokushima, Japan, in 1964, the M.Eng. and Dr.Eng. degrees from Kyoto University, Kyoto, Japan, in 1966 and 1974, respectively, all in electrical engineering. Presently, he is a Professor of Electrical and Electronic Engineering, Tokushima University, Tokushima, Japan. His interest is qualitative properties of nonlinear circuits.

erties of nonlinear circuits.